

## Influence of Failure Strain of Different Aluminium Alloys on Dynamic Problems

Marcos RODRIGUEZ-MILLÁN<sup>1)</sup>, Álvaro VAZ-ROMERO<sup>1)</sup>,  
José Antonio RODRIGUEZ-MARTINEZ<sup>1)</sup>, Alexis RUSINEK<sup>2)</sup>,  
Ángel ARIAS<sup>1)</sup>

<sup>1)</sup> *University Carlos III of Madrid*  
*Department of Continuum Mechanics and Structural Analysis*  
Avda. De la Universidad 30, 28911 Leganés, Madrid, Spain  
e-mail: mrmillan@ing.uc3m.es

<sup>2)</sup> *National Engineering School of Metz (ENIM)*  
*Laboratory of Mechanic, Biomechanic, Polymers and Structures (LaBPS)*  
1 route d'Ars Laquenexy, 57078 Metz Cedex 3, France

In this work an experimental-numerical methodology is devised for analyzing ductile fracture of two aluminum alloys under different values of stress triaxiality ( $0.2 \leq \eta \leq 1.2$ ) and Lode parameter ( $-1 \leq \mu \leq 0$ ). The experiments developed include combined loading (tension-torsion) tests on same NT specimen geometry for A 5754-H111 and AA 6082-T6. Numerical analysis shows that this type of specimen exhibits uniformity stable values of stress triaxiality and Lode parameter as plastic strain develops. Experimental results can be used to compare failure strain corresponding to different stress states. Moreover, to consider the influence of stress state in failure mechanics under impact loads, perforation tests of aluminum alloys have been developed in a range of impact velocity between  $120 \leq v \leq 500$  m/s. The tests were carried out with three different shape projectiles: conical ( $m = 29.4$  g) and two blunt ones ( $m = 29.4$  g and  $m = 1.1$  g). Results show the dependence on energy absorption with stress state and failure strain.

**Key words:** ductile failure, stress triaxiality, Lode parameter, aluminum, perforation.

### 1. INTRODUCTION

Aluminium alloys are used in numerous engineering fields like aeronautical, naval of automotive industry. A desirable requirement for an optimal design is mainly a high capacity for energy absorption in high loading rate events and a reducing of weight.

For a reliable prediction of the structural element behaviour and its energy absorption capacity until breakage, the numerical tools have to consider failure

criteria for the material. The simulation of such structures subjected to impact loads requires suitable constitutive laws capable of reproducing the material behaviour and representative failure models in the extreme conditions to which the component is subjected.

Pioneer works of MCCLINTOCK [1] and subsequently RICE and TRACEY [2] firstly introduced an important parameter, stress triaxiality  $\eta$ , which is defined as the ratio of hydrostatic pressure to Von Misses equivalent stress  $\sigma_e$ , Eq. (1.1).

$$(1.1) \quad \eta = \frac{\frac{1}{3}(\sigma_1 + \sigma_2 + \sigma_3)}{\sigma_e}.$$

A few years ago, several researchers [3, 4] have shown that the stress triaxiality alone is not sufficient to describe properly the behavior of the material at failure. Hence, the model developed by XUE and WIERZBICKI [5] considers the effect of the third stress invariant. The Lode parameter plays the role of third stress invariant, Eq. (1.2).

$$(1.2) \quad \mu = \frac{2\sigma_2 - \sigma_1 - \sigma_3}{\sigma_1 - \sigma_3}.$$

Recently, other fracture criterion has been proposed by STOUGHTON and YOON [6]. This criterion considers that fracture occurrence is predicted by the magnitude of maximum shear stress, although the influence of hydrostatic pressure is not considered in this one. In this regard, adequate damage models relate failure strain to stress triaxiality and Lode parameter. In general, calibration of these models has traditionally relied on specimens that exhibit high triaxiality and limited Lode parameter. This work presents a procedure that combines tension and torsion to achieve values of stress triaxiality ( $0.2 \leq \eta \leq 1.2$ ) and Lode parameter in the following range:  $-1 \leq \mu \leq 0$ . The existence of different stress states and failure modes is characteristic of dynamic process like collision events or perforation processes. In order to consider the influence of triaxiality and Lode parameter in those processes, perforation tests have been carried out in this work. Different shapes of projectile that modify the failure mode have been used.

## 2. COMBINED TENSION (COMPRESSION)-TORSION TEST

### 2.1. Procedure

Experimental tests were performed on circumferentially double notched tube specimen [4], Fig. 1. Tests were carried out in an universal servo-hydraulic machine which was adapted for this investigation, Fig. 2. This machine allows getting axial and torsional maximum values of 25 kN and 900 Nm, respectively. Tests were registered by Axial/Torsional Extensometer and optical camera.

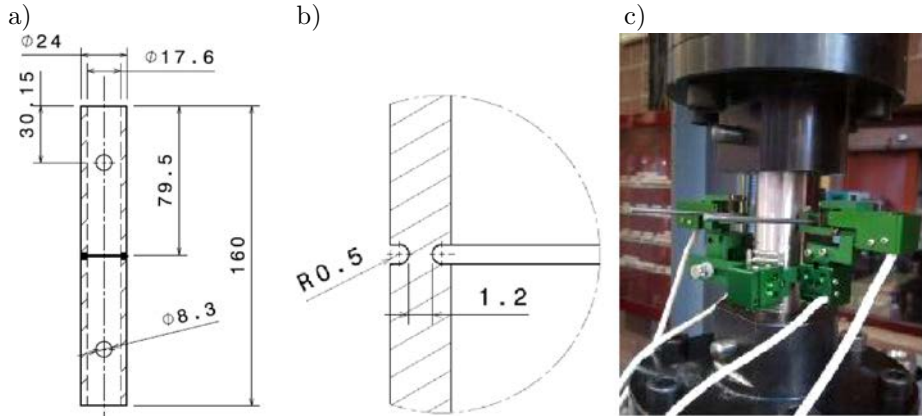


FIG. 1. a) Configuration of double notched tube specimen and b) zoom of the notch, c) Axial/Torsional Extensometer.

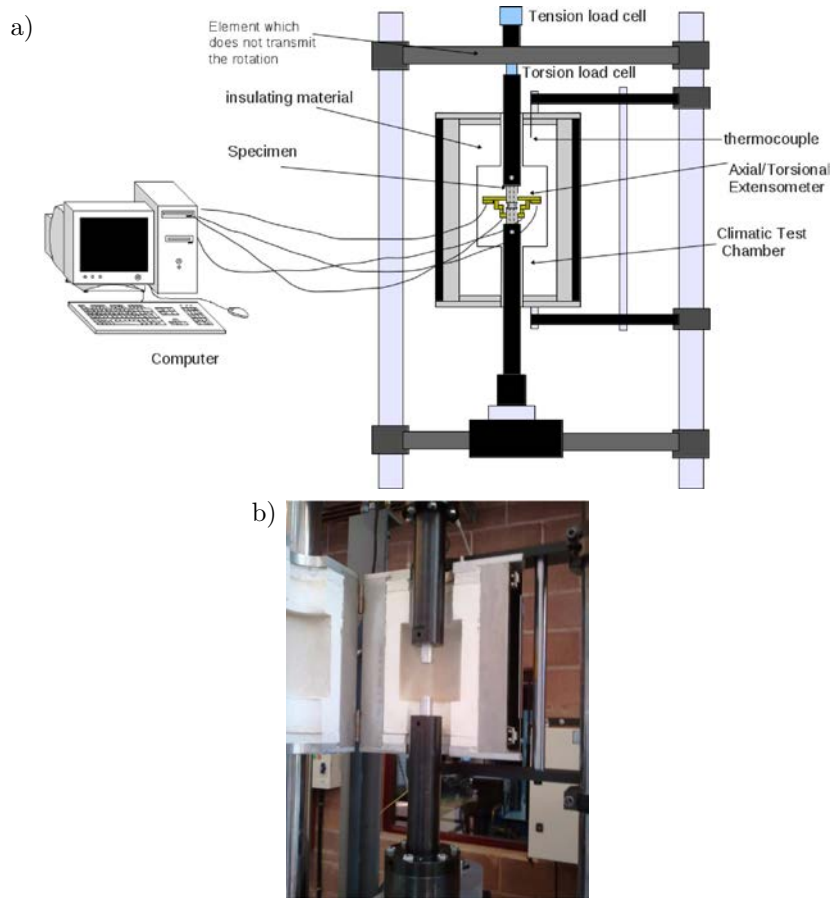


FIG. 2. a) Illustration of experimental machine, b) experimental universal servo-hydraulic machine.

The specimen is subjected to a combination of tensile and torsional loading using a load ratio parameter,  $\kappa$ , which is constant during the test, Eq. (2.1).

$$(2.1) \quad \kappa = \frac{\sigma_n}{\tau_n} = \frac{N \cdot r_m}{M},$$

where  $N$  is the axial force,  $M$  is the torsional moment and  $r_m$  is the value of radius to the centre of the notch.

A combined experimental-numerical methodology for analysing the influence of stress state in strain failure in the low to intermediate stress triaxiality regime has been implemented (Fig. 3). Main steps are:

- Procurement of load-displacement curves outside the notched zone by several experimental tests.
- Processing all tests using a two-dimensional (2D) model in finite element program ABAQUS, Figs. 4, 5.
- Determination and comparison the average effective strain. Experimental data results validate numerical simulations, Fig. 6.

Thus, stress and strain values calculated from simulations can be used to obtain the equivalent plastic failure strain and the stress triaxiality and Lode parameter.

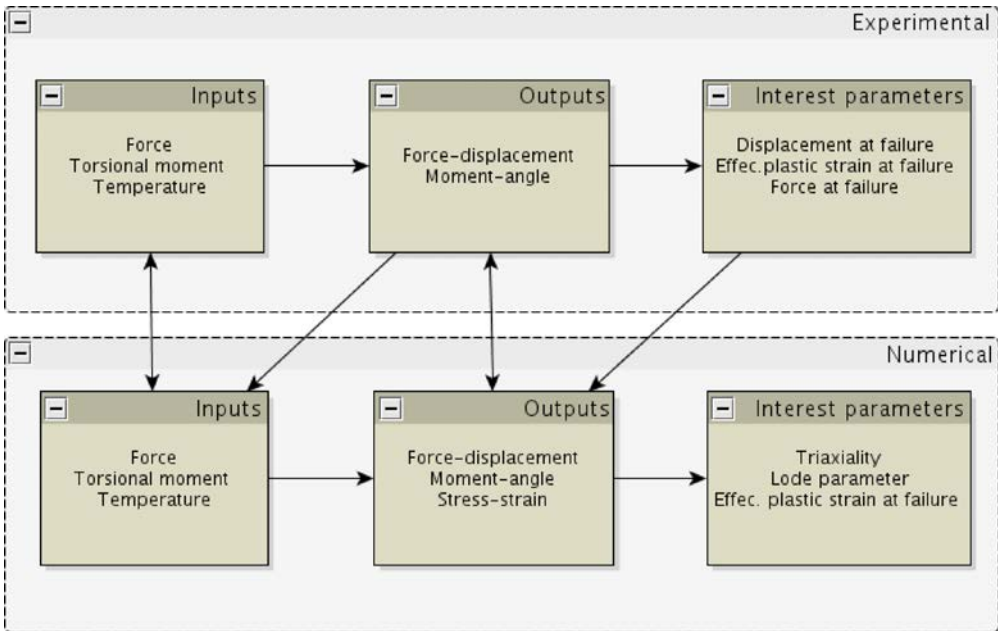


FIG. 3. Schematic methodology in order to perform combined tension-torsion tests.

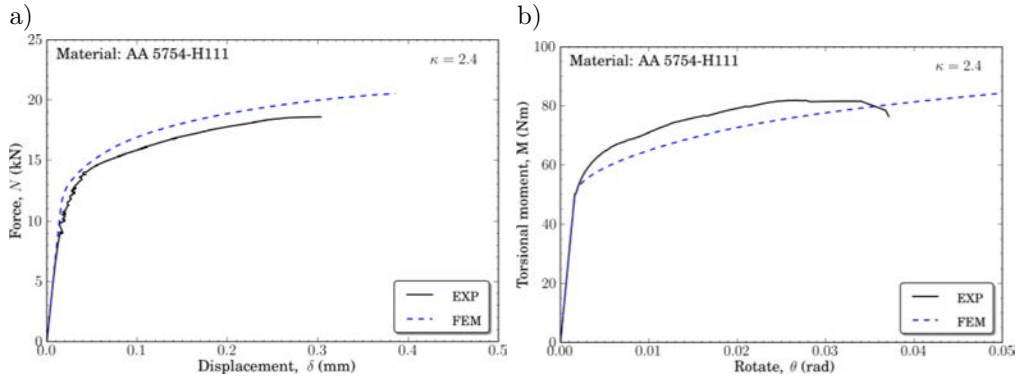


FIG. 4. Comparison between finite element simulations and experimental results for the aluminium 5754-H111 and  $\kappa = 2.4$ : a) axial force *versus* axial displacement, b) torsional moment *versus* angle rotation.

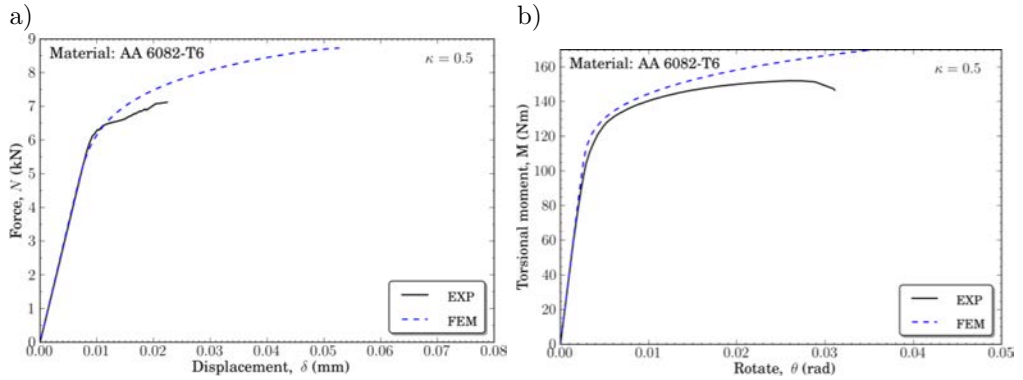


FIG. 5. Comparison between finite element simulations and experimental results for the aluminium 6082-T6 and  $\kappa = 0.5$ : a) axial force *versus* axial displacement, b) torsional moment *versus* angle rotation.

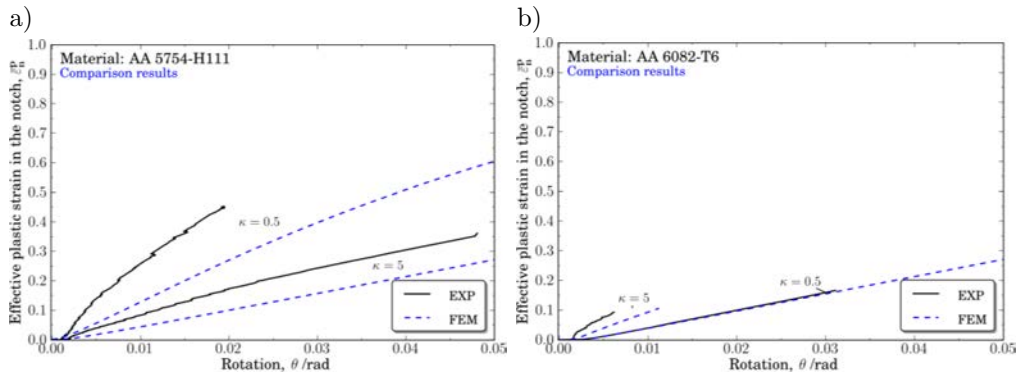


FIG. 6. Comparison between finite element simulations and experimental results. Effective plastic strain *versus* rotation for: a) the aluminium 5754-H111 and b) the aluminium 6082-T6.

## 3. RESULT ANALYSIS

From finite element simulations, the range in stress triaxiality is examined using the load ratio which varied from pure shear ( $\kappa = 0$ ) to pure tension ( $\kappa = \infty$ ). The maximum stress triaxiality value achievable is within the range  $0.9 \leq \eta \leq 1.22$ , Fig. 7a. The dependence of Lode parameter with respect to the stress triaxiality is illustrated in Fig. 7b. Data shows three distinct regions corresponding to different stress states: at low and high stress triaxiality, the stress state is approached to generalized shear ( $\mu \rightarrow 0$ ) and between them the stress state is approached to generalized tension ( $\mu \rightarrow -1$ ). The numerical analyses of the specimen show stable values of triaxiality and Lode parameter during the load history which is a desirable characteristic before failure, Fig. 7c.

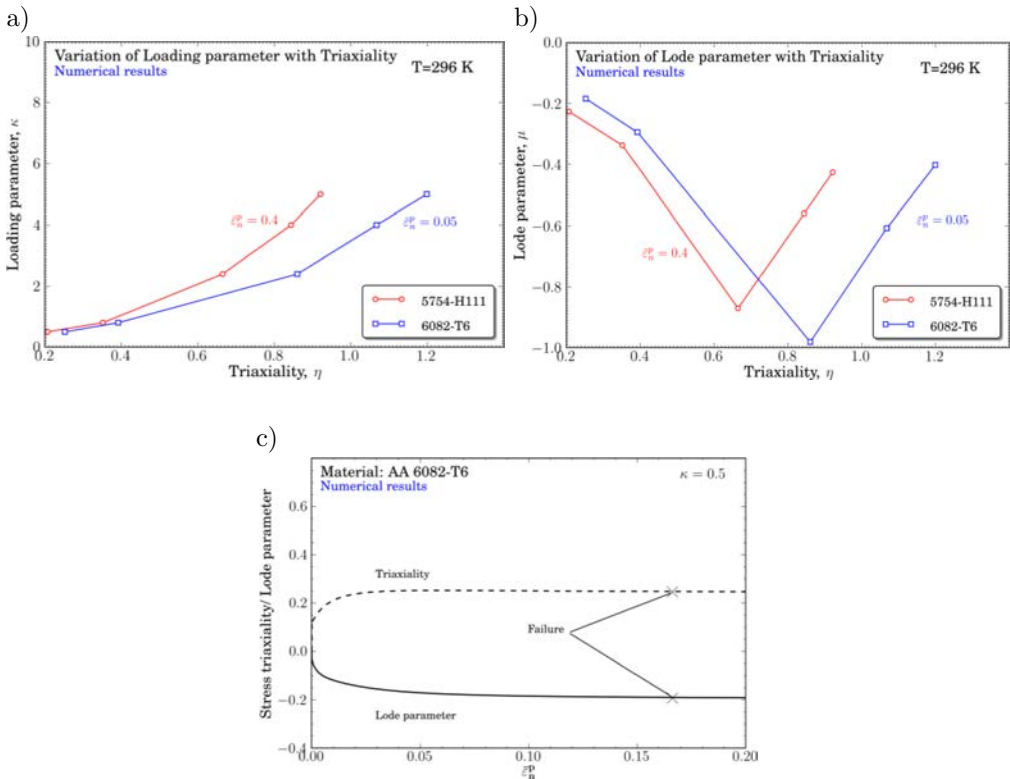


FIG. 7. a) Curve of Load parameter with stress triaxiality, b) comparison of Lode parameter and stress triaxiality over the range of applied loading conditions, c) evolution of stress triaxiality and Lode parameter in the centre of the notch.

The spatial variation of stress triaxiality, Lode parameter and the effective plastic strain is examined in Fig. 8b. The failure is marked by a sudden load

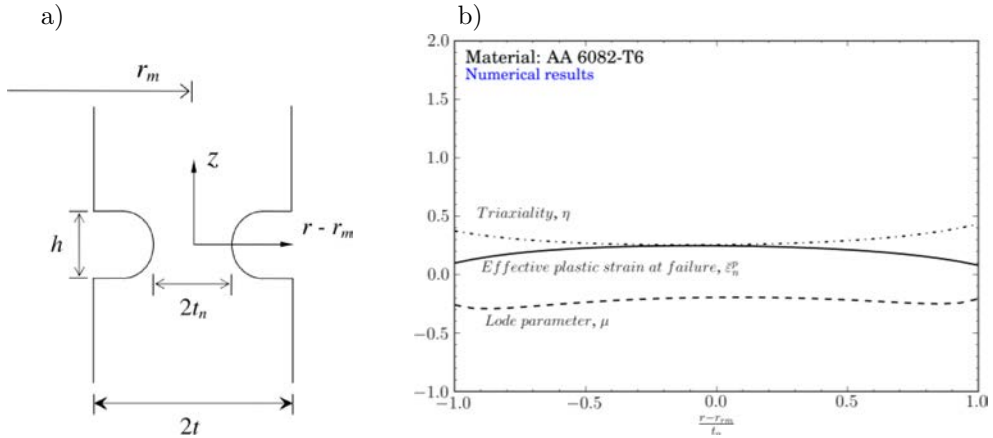


FIG. 8. Axisymmetric cut of notch (a) and b) through-thickness distribution of stress triaxiality, Lode parameter and effective plastic strain at the mid-section of the specimen.

drop which it is assumed in the centre portion of notch. In this regard, these parameters are explored in the symmetry plane ( $z = 0$ ) according to Fig. 8a.

A comparison of effective plastic strain at failure *versus* stress triaxiality and Lode parameter between aluminium alloys AA 5754-H111 and AA 6082-T6 is shown in Table 1. Data show a dependence on failure strain and stress triaxiality,  $\eta$ , and Lode parameter,  $\mu$ .

**Table 1.** Value of effective plastic strain at failure, stress triaxiality  $\eta$ , and Lode parameter,  $\mu$ , for AA 5754-H111 and AA 6082-T6.

	AA 5754-H111		AA 6082-T6	
	$\kappa = 0.5$	$\kappa = 5$	$\kappa = 0.5$	$\kappa = 5$
$\bar{\epsilon}_p^f$	0.361	0.452	0.166	0.092
$\eta$	0.206	0.916	0.246	1.187
$\mu$	-0.222	-0.405	-0.193	-0.377

To consider the influence of stress state in failure modes of dynamic processes, perforation tests have been performed.

#### 4. PERFORATION PROCESS OF ALUMINIUM PLATES

An analysis of ductile failure mechanics has been developed on AA 5754-H111 and AA 6082-T6 plates using three different projectiles: one conical ( $m_c = 29.4$  g) and two blunt ones ( $m_{b1} = 29.4$  g and  $m_{b2} = 1.1$  g). In total, 20 tests were performed.

Figure 9 shows energy absorbed by the plate as a function of the impact velocity. As is generally known, the projectile shape is an important param-

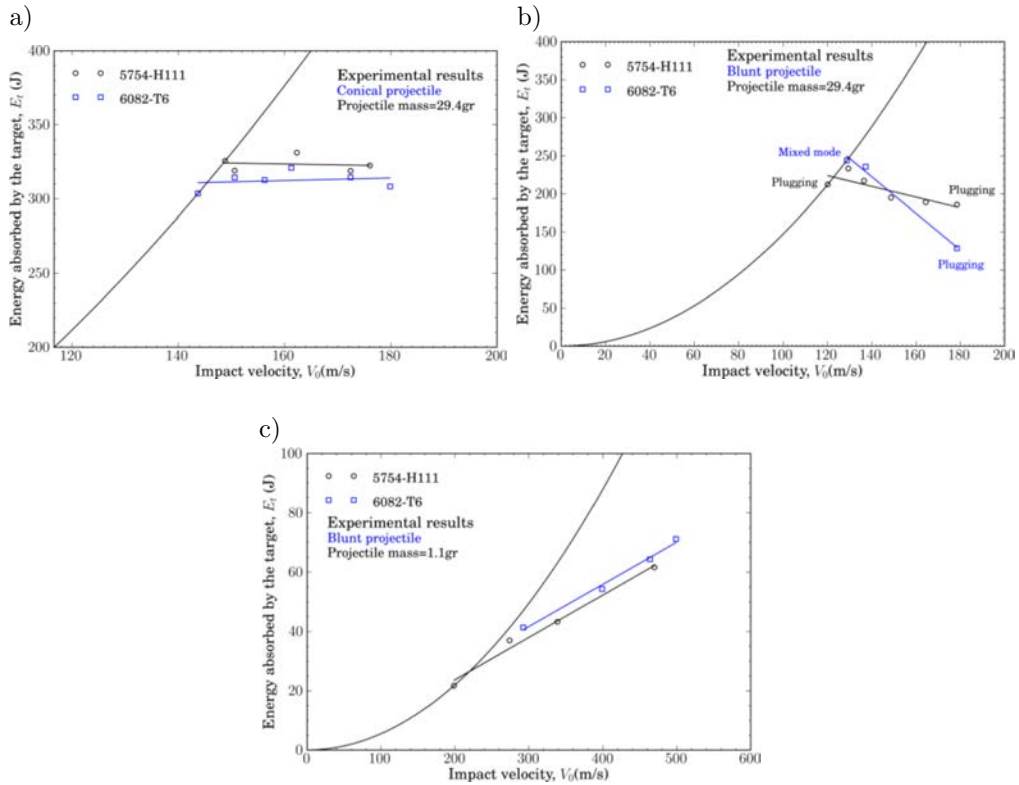


FIG. 9. Energy absorbed vs. impact velocity with a) conical ( $m = 29.4$  g), b) blunt ( $m = 29.4$  g) and c) blunt ( $m = 1.1$  g) projectile

ter in the perforation behaviour of the plate. The experiments performed with same conical projectile and mass ( $m = 29.4$  g) revealed that energy absorption is approximately constant, Fig. 9a. In this case, petalling failure mechanics is produced by high radial and circumferential tensile stress. As a result, the tests revealed that for both aluminium alloys the energy absorption capacity was similar. This result is coherent with failure strain value obtained for these materials, Table 2.

**Table 2.** Value of tensile and shear strain for AA 5754-H111 and AA 6082-T6.

	AA 5754-H111	AA 6082-T6
$\varepsilon_f$	0.172	0.170
$\gamma_f$	0.379	0.32

However, it can be observed a significant decreasing in energy absorption with the increase of impact velocity when a blunt projectile is used, Fig. 9b.

Moreover, the perforation mechanics was markedly different. Plugging failure is due to adiabatic shearing. AA 6082-T6 shows less energy absorption ( $E_a = 120$  J) than AA 5754-H111 ( $E_a = 200$  J), according to failure shear strain values in Table 2. This behaviour can be explained by the more sensibility of AA 6082-T6 to localize plastic deformation in conditions of low stress triaxiality and consequently the minor plastic work developed for plate explain of decreased absorption energy. Experimental data obtained (Table 1) show minor value of failure strain of AA 6082-T6 at low values of  $\kappa$  (*shear states*). Moreover, the impact experiments were carried out with another mass projectile and same blunt shape, in order to compare the energy absorption, Fig. 9c.

## 5. CONCLUSIONS AND REMARKS

In this work, a procedure for estimation of the effective plastic strain and characterization of stress state at failure has been developed. The methodology allows a control of stress triaxiality and Lode parameter by a fixed loading ratio. In addition, for considered aluminum alloys, the effect of stress state on failure strain and energy absorption has been evaluated on perforation tests.

## REFERENCES

1. MCCLINTOCK F.A., *A Criterion for Ductile Fracture by the Growth of Holes*, Journal of Applied Mechanics, **35**, 363–371, 1968.
2. RICE J.R., TRACEY D.M., *On the Ductile Enlargement of Voids in Triaxial Stress Fields*, Journal of the Mechanics of Physical Solids, **17**, 201–217, 1969.
3. BAO Y., WIERZBICKI T., *On Fracture Locus in the Equivalent Strain and Stress Triaxiality Space*, International Journal of Mechanical Sciences, **46**, 81–98, 2004.
4. BARSOU M., FALESKOG J., *Rupture Mechanisms in Combined Tension and Shear – Experiments*, International Journal of Solids and Structures, **44**, 1768–1786, 2007.
5. XUE L., WIERZBICKI T., *Ductile fracture initiation and propagation modeling using damage plasticity theory*, Engineering Fracture Mechanics, **75**, 11, 3276–3293, 2008
6. STOUGHTON T.B., YOON J.W., *A new approach for failure criterion for sheet metals*, International Journal of Plasticity, **27**, 3, 440–459, 2011.

*Received May 25, 2012; revised version October 9, 2012.*

---